Chapter 11

Collective Excitation Phenomena and their Applications

David Horn and Irit Opher
School of Physics and Astronomy
Raymond and Beverly Sackler Faculty of Exact Sciences
Tel Aviv University, Tel Aviv 69978, Israel

11.1 Introduction

Spiking neurons are highly non-linear oscillators. As such they display collective behavior that may have important calculational manifestations. Synchronization between the firing of different neurons is the first topic to which we devote our attention. This behavior can be brought about in our integrate-and-fire model through excitatory synaptic couplings without delays, or inhibitory couplings with delays. Once the mechanism of synchronization is established, this phenomenon can be used for defining data clustering. The clusters correspond to neurons that fire synchronously, with different clusters firing at different times. This behavior can also be described as temporal segmentation, separating data through phase lags between excitations of different aggregates. This separation is characteristically limited to a small number of segments, a limitation that is inherent to the behavior of coupled non-linear oscillators.

The importance of synchrony as signifying binding, i.e. the belonging of neural events to one another and their joint formation of a consistent picture or concept, was emphasized by von der Malsburg [von der Malsburg, 1981]. Experiments in the late 80's [Eckhorn *et al.* , 1988, Gray *et al.* , 1989] showed the correlation of synchrony in the visual cortex with binding in the input scene. Taking it one step further, one may ask for the co-occurrence of several synchronized neuronal assemblies. This could explain distributed attention [von der Malsburg and Schneider, 1986]. It was studied in various neural models [Wang, Buhman and von der Malsburg, 1990, Horn and Usher, 1991, Horn, Sagi and Usher, 1991] but has no experimental verification.

Employing quasi-local excitatory connections one can use these principles for image analysis. After covering cluster formations we turn to the use of an image as an external input to a two dimensional array of spiking neurons, and demonstrate how we can perform edge detection as well as scene segmentation. Finally, we study spatio-temporal coherent phenomena that homogeneous neural systems may develop by themselves. We show how solitary waves of spiking activity arise on neuronal surfaces, and characterize their structures.

In order to demonstrate the various concepts and phenomena we use our continuous version [Horn and Opher, 1997a] of integrate-and-fire (IAF) neurons, that were discussed in section 1.2.3.3. of chapter 1. We employ a coupled set of differential equations of two variables, as described in the next subsection.

11.1.1 Two variable formulation of IAF neurons

The two variables that we use to describe an IAF neuron are v, a subthreshold potential, and m which distinguishes between two different modes in the dynamics of the single neuron, the active depolarization mode and the inactive refractory period. They obey

$$\dot{v} = -kv + \alpha + cmv + mI \tag{11.1}$$

$$\dot{m} = -m + \Theta(m - v) \tag{11.2}$$

$\Theta(x)$ is the Heaviside step function. The neuron is influenced by an external input I, which is quenched in the absolute refractory period, when $m = 0$. Starting out with $m = 1$, the total time derivative of v is positive, and v follows the dynamics of a charging capacitor. Hence this represents the depolarization period of v. During all this time, since $v < m$, m stays unchanged. The dynamics change when v reaches the threshold (that is arbitrarily set to 1). Then m decreases rapidly to zero, causing the time derivative of v to be negative, and v follows the dynamics of a discharging

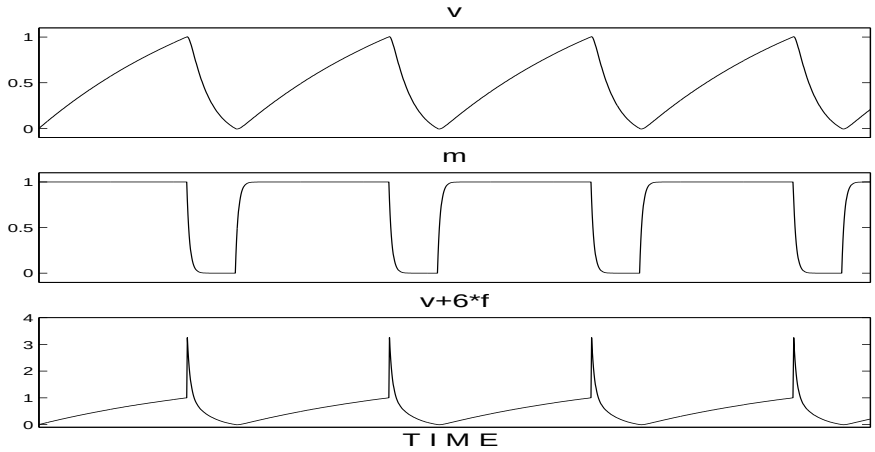

Figure 11.1: Dynamics of the single IAF neuron. The upper frame displays v, the subthreshold membrane potential, as a function of time. The second frame shows m, the variable that distinguishes between the depolarization state, $m = 1$, and refractoriness, $m = 0$. In the third frame we plot $v + 6f$, where f is our spike profile, to give a schematic presentation of the total cell potential. Parameters for this figure are: $k = 0.45$, $\alpha = -0.09$, $c = 0.35$, $I = 0.29$.

capacitor. Parameters are chosen so that the time constants of the charging and discharging periods are different.

To complete this description of an IAF neuron we need a quantity that represents the firing of the neuron. We introduce for this purpose

$$f = -\frac{dm}{dt}\theta(-\frac{dm}{dt}) \tag{11.3}$$

that vanishes at all times except when v arrives at the threshold and m changes rapidly from 1 to 0. This can serve therefore as a description of the action potential. An example of the dynamics of v and m is shown in Fig. 11.1. In a third frame we plot $v + af$, with $a = 6$, representing the total soma potential. The value of a is of no consequence in our work. It is used here for illustration purposes only.

This description can be readily extended to an array of pulse coupled neurons by replacing Eq. 11.1 with

$$\dot{v_i} = -kv_i + \alpha + cm_iv_i + m_i(I + \Sigma_j w_{ij} f_j) \tag{11.4}$$

where $i = 1, \cdots, N$ denotes the number of the neuron. Note that in this formulation the interactions are instantaneous, and are quenched during the refractory period,

when $m_i = 0$. It is straightforward to introduce neuritic time delays, e.g. by switching $f_j = f_j(t)$ to $\bar{f}_j = f_j(t - \Delta)$ on the right hand side of this equation. One should note that the spike, represented here by f, has some width of its own, so a small effect of temporal extension is embedded automatically in the definition of our model.

11.2 Synchronization of Pulse Coupled Oscillators

Synchrony of events is an intriguing physical phenomenon. The fact that most living organisms depend upon it for their survival makes it even more interesting. Synchronization plays an important role in many physiological activities including breathing, motor control and information processing in the central nervous system. It can also occur in biological environments that include many organisms such as groups of fireflies that flash in synchrony or groups of criquets chirping in unison [Strogatz and Stewart, 1993].

Most biological systems that exhibit synchronization can be described as coupled oscillators, where the fully synchronized state is only one of many possible dynamic attractors. One can divide models of coupled oscillators into two kinds: phase coupled [Golomb *et al.* , 1992, Grannan, Kleinfeld and Sompolinsky, 1993, Terman and Wang, 1995] and pulse coupled ones [Mirollo and Strogatz, 1990, Hopfield and Herz, 1995, Johnson, 1994]. The latter reduces to the former in the limit in which every oscillator couples to a large number of others [Abbott and van Vreeswijk, 1993, Kuramoto, 1990, Gerstner, Ritz and van Hemmen, 1993, Usher, Schuster and Niebur, 1993]. We will devote our attention to pulse coupled systems, analyzing cases of both small and large numbers of neurons.

In this chapter we address collective activity in neuronal populations with various types of coupling. In this section, we concentrate on all-to-all couplings. This will serve as the basis for understanding cases in which the synaptic couplings reflect structure in data or the geometry of a manifold to which neurons are attached. A thorough analysis of the large N limit of such systems is given in Chapter 10. Let us start with all-to-all excitatory couplings, a case studied by [Mirollo and Strogatz, 1990]. They considered a population of N identical pulse coupled oscillators, fully connected by excitatory connections, without transmission delays and with no refractory period. The state of the single oscillator is described by a monotonic increasing function of its phase, representing the integration that the membrane potential performs over its inputs. Once an oscillator reaches its threshold it emits a spike and is

automatically reset to zero. Under the simple assumption that the monotonic function is concave, the authors prove that for almost all initial conditions the neuronal population will reach a stable synchronized state after a finite number of time steps, for any value of N. In the case of inhibitory connections they show that for a system of 2 neurons, the asynchronous solution is stable. Although they do not prove it for a larger system, this result is supported by numerical simulations and by other models, as will be shown below.

The situation is quite different when transmission delays are added to such a model. Nischwitz and Glünder [Nischwitz and Glünder, 1995] report that, for a wide range of parameters, transmission delays cause desynchronization. However, if excitatory connections are replaced by inhibitory ones, transmission delays induce synchronization. Following a numerical study, they conclude that delayed local inhibition is the best scheme for spike synchronization. This conclusion agrees with [van Vreeswijk and Abbott, 1994], who studied a system of two integrate and fire units interacting through a dynamic synapse described by an α function. They showed that while the synchronous state is not stable for an excitatory synapse, it is stable when the synapse is inhibitory. In fact, the synchronous state is always stable when the synapse is inhibitory, although its domain of attraction shrinks as the interaction becomes faster. In the excitatory case, the stable synchronous state is reached only when the interaction is instantaneous.

Whereas in our model synaptic response is instantaneous, and neuritic delays are introduced at will, realistic models cope with both synaptic and neuritic temporal structures, leading to various effects. As an example let us mention [Hansel, Mato and Meunier, 1995], who study realistic neural models using both analytic calculations (after reduction to a phase model) and numerical simulations. They differentiate between two types of responses to excitatory post-synaptic potentials (EPSP). In the first case, the EPSP advances the next firing of the excited neuron. In the second case, it can either delay the spike or advance it, depending on the arrival time of the EPSP relative to the refractory period. A synchronized state is not stable in the first scenario[1], while it can be stable in the second one, provided the synaptic interactions are fast enough.

The importance of the timing of a spike is further emphasized in the locking theorem of [Gerstner, van Hemmen and Cowan, 1996] (see section 10.2.5.2). It states the conditions for stability of the fully synchronous solution in a more complex case (the spike response model introduced in section 1.2.3.1 of chapter 1) that incorporates the form of the post-synaptic potential as well as axonal delays and refractoriness.

[1]It may, however, be stable for instantaneous synapses.

Collective firing is shown to be stable if the firing occurs while the post-synaptic potential is rising.

In the more simplistic models, including ours, the general conclusion is that both instantaneous excitation and delayed inhibition can lead to synchrony. Instantaneous excitation has the advantage that synchrony follows quickly once the interaction is strong enough. In the case of delayed inhibition one has to find the correct window of parameters and wait longer for synchrony to set in, but once it is obtained it is very stable. Recent studies [Crook, Ermentrout and Bower, 1997, van Vreeswijk and Hansel, 1997] have shown that synaptic adaptation has an interesting effect: it leads to synchrony of spiking neural systems in the presence of excitatory synaptic interactions with realistic temporal structures. Thus, once we allow for more elaborate interactions, there exist many ways of inducing synchrony.

We illustrate in Fig. 11.2 the build-up of synchrony in our system of IAF neurons [Horn and Opher, 1997a] for different types of interactions. For all-to-all excitatory instantaneous couplings we display a system of neurons that starts out with random initial conditions and turns, after four periods, into a synchronous system. When the interactions are inhibitory, the system is periodic but asynchronous. Finally, inhibition with fixed transmission delays leads to the build-up of synchrony through merger of synchronous clusters.

In discrete temporal simulations, there exists a subtlety regarding the exact updating scheme. One can either reset the IAF neuron to its rest state, no matter how much current it received before firing, or to a higher value, if the input it received before firing exceeded the amount it needed to reach threshold. When refractoriness is present, as is the case in our model, the situation is similar to the first updating scenario. It becomes the only possible one, since current that arrives during and immediately after the spike cannot drive the neuron to fire.

Throughout this chapter we discuss systems of IAF neurons whose interactions depend on some underlying geometrical structure. Once we allow for deviations from all-to-all couplings, new interesting phenomena develop. Hopfield and Herz [Hopfield and Herz, 1995] have investigated several types of models in which each neuron is excitatorily connected to four nearest neighbors on a two dimensional grid. They find that all models exhibit rapid convergence to cyclic solutions, although not all solutions are globally synchronous. Their two models of leaky IAF neurons reach either global synchrony or a state of phased locked oscillations, i.e. a number of synchronized clusters of neurons, where the different clusters are phase shifted with respect to each other. Each cluster contains at least one triggering neuron and its nearest neighbors. The authors show that the type of cyclic attractor depends on

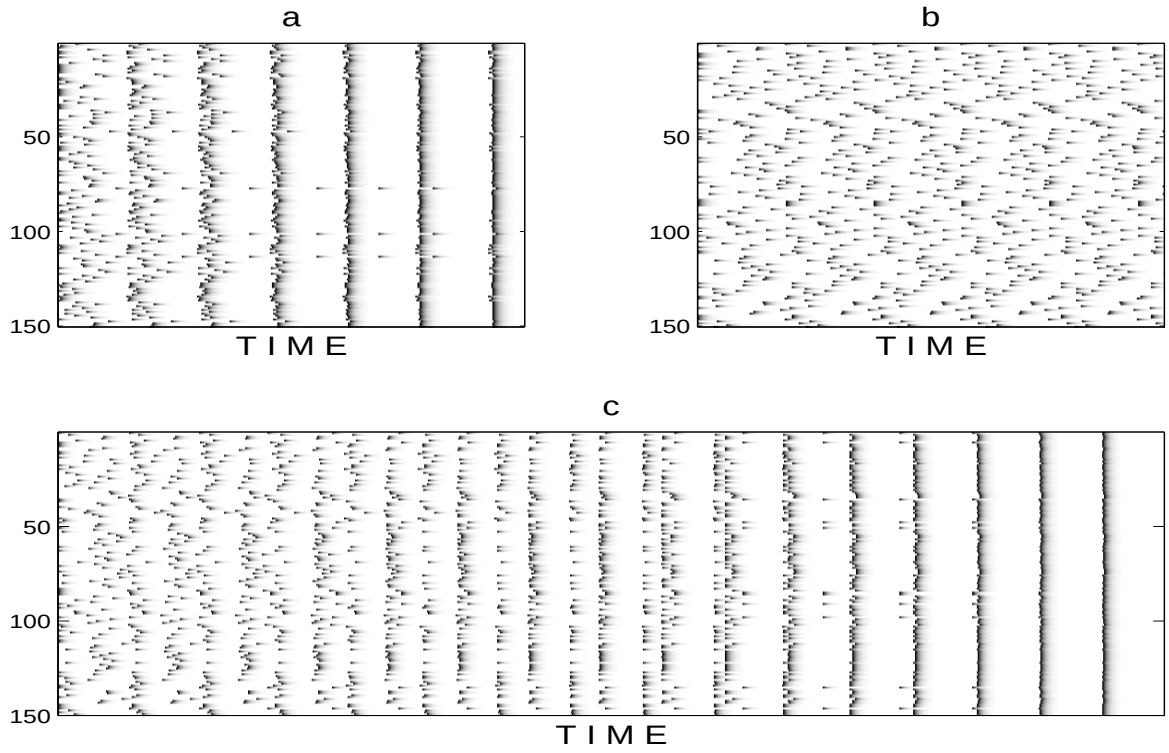

Figure 11.2: Firing of 150 IAF neurons with all-to-all interactions vs. time. Starting from random initial conditions, the global behavior depends on the connections:
(a) Excitatory connections without delay lead quickly to almost perfect synchronization. (b) In the presence of inhibitory connections without delay, the system converges to non-synchronized periodic behavior. (c) Delayed inhibition inducing perfect synchronization after a long time.

the updating scheme chosen for the model. They conclude that spatially connected networks exhibit richer collective phenomena than globally connected networks. A discussion of spatiotemporal patterns that evolve in spatially connected networks will be presented in the last section. It is important to note that most of the systems discussed in this chapter are composed of neurons with the same internal period. Models of random intrinsic frequencies [Strogatz and Mirollo, 1988] that exhibit other interesting dynamic behavior are beyond the scope of this chapter.

11.3 Clustering via Temporal Segmentation

Clustering is an important concept in data analysis [Duda and Hart, 1973]. When data are presented in some given space one may follow any one of a set of parametric approaches that exist in the literature. But if the space is very large, it is advantageous to concentrate not on the location of the data points but on the distances between them. In that case an analogy with a neural system may suggest itself, associating the data points with neurons and the distances with synaptic interactions between them. Such an approach was recently suggested in [Blatt, Wiseman and Domany, 1997], where the authors have applied methods of statistical mechanics to such a system, using the analogy of ferromagnetic interactions among spins. This leads to impressive results for a host of problems where, as a function of one parameter, the temperature, one can follow a tree of bifurcations into different clusters.

In the present section we demonstrate how a system of IAF neurons can be used to perform such a task, relying on the fact that coupled IAF neural systems can exhibit staggered oscillations of neuronal cell assemblies. These assemblies are defined through the synchrony of their neurons, and we use them to represent clusters. Typically we will be able to segregate data into sets of a few clusters in this fashion. The limit on the possible number of clusters will be discussed in the next section.

Suppose we are given an $N \times N$ symmetric distance matrix, defined for N data points. For the solution of the clustering problem we have in mind, in which clusters are composed of groups of points, we define a set of symmetric synaptic connections among N IAF neurons, that are negatively correlated with distance. Thus short distances will imply strong excitatory interactions, and long distances may lead to inhibition. The neurons are assumed to be under the influence of some common input, so that, in the absence of interactions, they will behave like free non-linear spiking oscillators. When the interactions are turned on we obtain, in general, staggered oscillations of groups of neurons. These groups will be associated with the required clusters. To make sure that global synchronization will not be reached, competition between the different clusters can be induced by global instantaneous inhibition that is proportional to the total spiking activity. This turns Eq. 11.4 into

$$\dot{v_i} = -kv_i + \alpha + cm_iv_i + m_i(I + \Sigma_j w_{ij}\bar{f_j} - \gamma\Sigma_j f_j). \tag{11.5}$$

In the presence of such global inhibition, classification into clusters of roughly the same size is favored by this method. In the example of Fig. 11.3 we see clustering of 547 data points formed by slightly overlapping three gaussian distributions. We have used here inhibitory connections with delays (that lead to synchronization, as

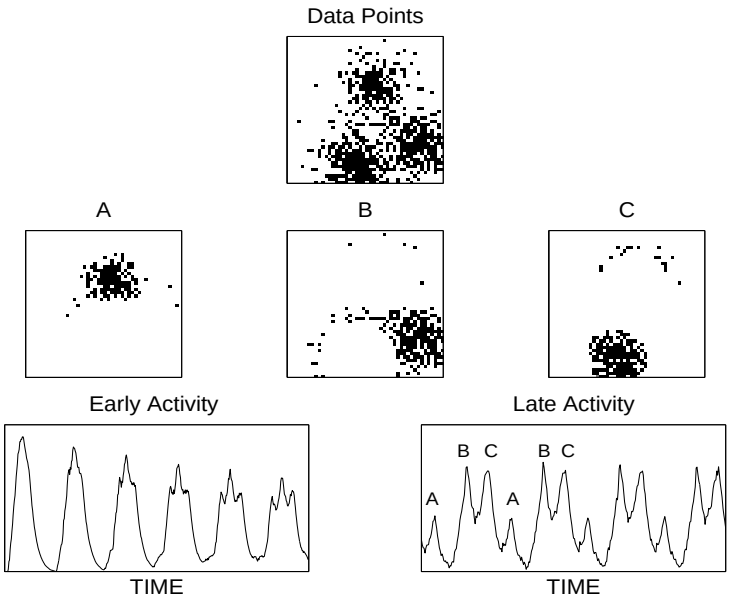

Figure 11.3: Clustering of 547 data points with a spiking system. The data points are shown in the upper frame. Each point is associated with an oscillatory neuron (same constant input). Initial conditions are all zero, and the interactions are defined according to the relative distances between the points. To induce synchrony we use delayed inhibition between all neuron pairs whose distance is below 6, with the delay time being roughly a third of the neuron's oscillation period. Competition is induced by global instantaneous inhibition. The two bottom frames show the total activity of the system, that starts out as a single synchronized state which later separates into three different peaks. Each peak corresponds to one of the clusters displayed in the middle frames.

shown in section 11.2) with an additional instantaneous global inhibition. The system converges onto a periodic solution of staggered oscillations. Each peak in the total activity (lower right frame) corresponds to one of the clusters, shown in the middle frames. Approximately 90% of the data points are classified correctly.

Clustering problems are often ill defined. Usually there are many partitions of the data that can qualify as clusters. Moreover, within a given method there may exist many solutions to a given problem. This is also the case in our method when the distance matrix is not as clearly structured as in the example given above. When faced with such a situation one may impose a constraint based on the assumption of simply connected topology of clusters, and require that the average distance within a cluster be smaller than the average distance to points in different clusters. This would of course fail for non-trivial topologies where the distance condition does not

hold. Examples of such problems were given in [Blatt, Wiseman and Domany, 1997].

Clustering becomes a complex problem when the number of data points is large. An exhaustive search for solutions, e.g. seeking groups of points that obey the distance condition, becomes computationally time consuming. Therefore one looks for heuristic methods to solve such problems. The advantages of our pulse-coupled system is that it relies only on distances between the points, it can be applied to problems of arbitrary size, and it does not require preprocessing that is problem specific . Its disadvantages are that it naturally leads to a small number of clusters, e.g. 3 or 4, independent of the size of the problem, and it is biased toward clusters of the same average size.

11.4 Limits on Temporal Segmentation

Clustering was achieved in the previous section via temporal segmentation. The fact that this method leads to a small number of clusters is characteristic of non-linear oscillators that perform staggered oscillations (e.g. [Hansel, Mato and Meunier, 1995, Golomb *et al.* , 1992]). This is readily observed in associative memory systems that are based on continuous oscillatory neurons [Wang, Buhman and von der Malsburg, 1990, Horn and Usher, 1991]. These models provide temporal segmentation into 3 to 6 components only. It is tempting to speculate that this feature could provide an explanation [Horn and Usher, 1992] for the known limits on short term memory such as Miller's 7 ± 2 rule [Miller, 1956].

To understand why one obtains the limit on segmentation we have studied a dynamical system composed of n continuous excitatory neurons interacting with one inhibitory neuron [Horn and Opher, 1996a]. Here each neuron, or oscillatory unit, can be thought of as representing a cell assembly of spiking neurons.

$$dU_i/dt = -U_i + M_i - aM^I - b\theta_i + I_i \tag{11.6}$$

$$d\theta_i/dt = M_i - c\theta_i \tag{11.7}$$

$$dU^I/dt = -gU^I - eM^I + f\sum_i M_i \tag{11.8}$$

U_i, for $i = 1, \cdots, n$ denote post-synaptic currents of excitatory neurons, whose average firing rates are

$$M_i = (1 + e^{-\beta U_i})^{-1} \tag{11.9}$$

while U^I and M^I are analogous quantities for an inhibitory neuron that induces competition between all excitatory ones. θ_i are dynamical thresholds that rise when their

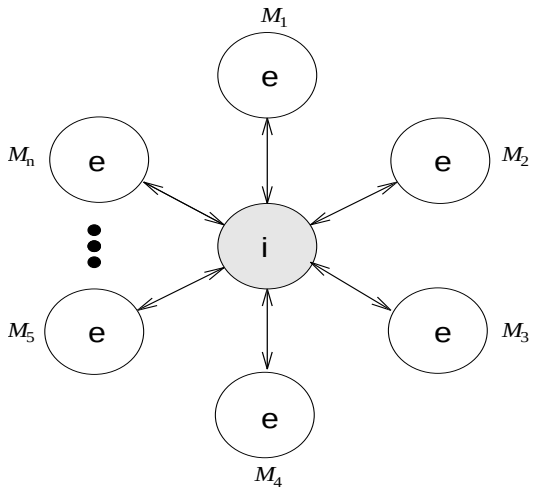

Figure 11.4: A schematic representation of a model of identical excitatory oscillators coupled to an overall inhibitory unit.

corresponding neurons i fire. They quench the active neurons and lead to oscillatory behavior. $a, \cdots, g$ and β are fixed parameters. To study segmentation we choose $I_i = I$ as a common external input, in which case the system becomes fully symmetric under the interchange of any two neurons $i \leftrightarrow j$. A schematic representation of the model is displayed in Fig. 11.4.

For a wide range of parameters this system can be shown to converge into limit cycles that include segmentation. However, full segmentation is obtained only up to $n = 5$. Above that, only partial segmentation can be obtained. An example of the latter is shown in Fig. 11.5. To understand why full segmentation cannot be obtained in this model for $n > 5$ we note that the overall period of the repeating pattern, τ, stays roughly the same, for all n. On the other hand a single oscillatory beat cannot be too narrow. Technically the limit follows from an analysis of the subharmonic oscillations of an excitatory unit in response to the input it receives from the inhibitory unit, which oscillates at a higher frequency due to the influence of all other oscillatory excitatory units. Narrow subharmonic oscillations are restricted to $n \leq 5$, thus providing the reason for the limit on full segmentation. Moreover, subharmonic oscillations of $n = 3$ are the most stable ones, which explains their dominance in partial segmentation patterns such as the one shown in Fig. 11.5.

This limitation can be overcome if one allows appropriate noisy inputs [Horn and Opher, 1996b]. We have worked with inputs of the type $I_i = 0.4 + 0.1\xi_i$, where ξ_i is a random variable between 0 and 1, that changes rapidly. For $n = 3$ this leads

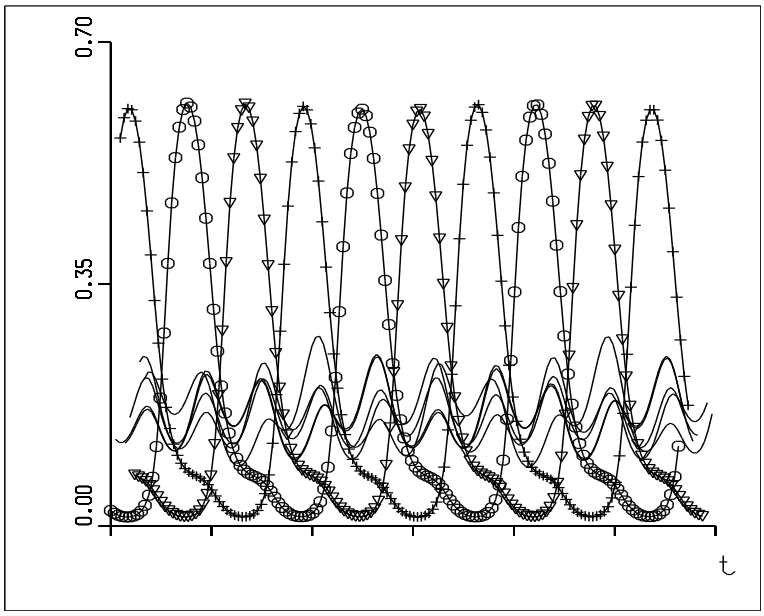

Figure 11.5: A quasiperiodic solution of the $n = 8$ problem that displays partial segmentation. The eight M values of the different oscillators are shown. The three large amplitudes form a segmented pattern, while the low amplitudes display very different periodicities.

to a regular structure of full segmentation. The symmetry is obtained in spite of the random component in the input. The interesting effect of noise in this system is to select full segmentation as the only surviving limit cycle. Increasing n to 4 and more, we find that all symmetrical structures are broken. The general pattern is one of approximate segmentation. For large n values ($n > 5$) simple noise does not induce full segmentation. There exists either large overlap between different oscillators (degenerate segmentation) or partial segmentation in a very disordered fashion. In order to obtain full segmentation one has to make sure that the (random) input affects no more than five oscillators at a time. We have therefore employed two random components. One assigns to each oscillator a random input, and the other selects the five oscillators that are allowed to have their input active at a given time. The two independent random sequences are chosen to have rapid variations, i.e. time scales less than 0.1τ. This type of input has a random Fourier decomposition. The results are displayed in Fig. 11.6. Segmentation is quite evident. The order of the dominant oscillators is random, yet, on the average, all oscillators are being excited. Our conclusion from this study is that for appropriate noise patterns, of the type described above, segmentation can be induced for any number of oscillators [Horn and Opher, 1996b].

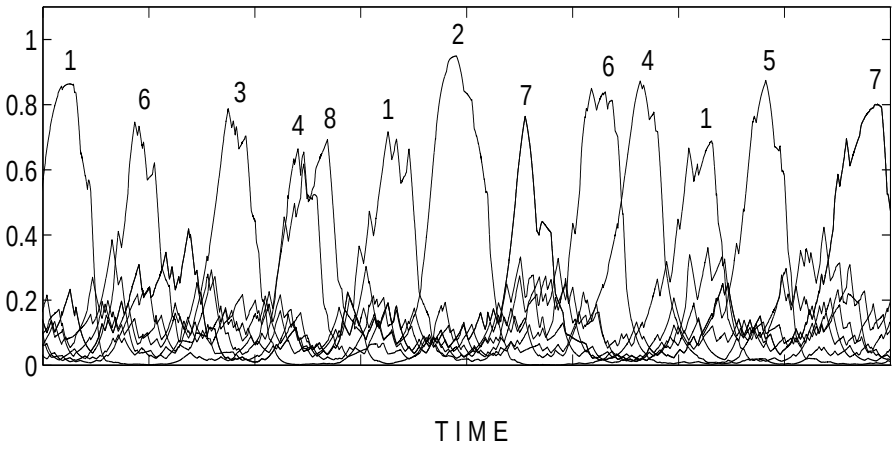

Figure 11.6: Staggered oscillation of the $n = 8$ problem is obtained for random inputs with rapid variation, affecting a few oscillators at a time. Activities of all oscillators are displayed as function of time.

11.5 Image Analysis

Analysis of a visual scene is one of the most difficult tasks performed by animal brains. It involves, among other sub-tasks, image segmentation, feature extraction and edge detection. Image analysis is also an important requirement of many artificial intelligence systems used in various fields from navigation to medicine. Great effort has been devoted towards inventing good algorithms for image analysis. However, an algorithm that does not require preprocessing (i.e. one that is not image specific) is hard to find. Therefore, as is the case in other AI implementations, it might prove useful to imitate biology, which is the best known performer of these tasks. This could be done via the temporal binding hypothesis suggested by von der Malsburg in 1981 [von der Malsburg, 1981, von der Malsburg and Schneider, 1986]. According to this idea, activities of neurons that correspond to the same feature are synchronized while representations of different features are temporally decorrelated. There exists evidence that such a strategy may be employed by the brain [Eckhorn *et al.* , 1988, Gray *et al.* , 1989].

Examples of the implementation of this idea in an oscillatory neural network for segmentation and binding exist in the literature [Wang, Buhman and von der Malsburg, 1990, Horn, Sagi and Usher, 1991, von der Malsburg and Buhman, 1992, Johnson, 1994, Ritz *et al.* , 1994, Horn and Opher, 1996a, Wang and Terman, 1997]. All these models share some interesting features. One of these is the necessity of competition between the different oscillators, usually in the form of global inhibition,

allowing only a small number of oscillators to rise simultaneously. Another common feature is the limited segmentation ability. In most models, only a small number of objects can be segmented. This ties in with the limit on temporal segmentation that we discussed before.

11.5.1 Image segmentation

The phenomenon of clustering, and the fact that we have a neural computational mechanism to achieve it, can be employed to perform image segmentation. For this purpose let us embed IAF neurons on a regular two dimensional surface with open boundary conditions. Each neuron is being fed an input whose amplitude corresponds to the grey scale of a pixel of a given image. The problem of segmentation is to define clusters that represent different objects in the image. The simplest way of clustering is to rely on similarity in the grey scale within some given radius. Hence it is natural to define an input dependent interaction that leads to mutual excitations between neurons that receive similar inputs, and to mutual inhibition between those that have very different inputs. This can be achieved through the following choice:

$$w_{ij} = F\left(\frac{1}{1+|I_i - I_j|}\right)\Theta\left(d_{max} - d_{ij}\right) \tag{11.10}$$

$$F(x) = \begin{cases} \frac{2}{\theta^2}\left(x^2 - x\theta\right) & x \leq \theta \\ \frac{1}{1-\sqrt{\theta}}\left(\sqrt{x} - \sqrt{\theta}\right) & x \geq \theta \end{cases} \tag{11.11}$$

where $\theta = \frac{1}{1+0.5(I_{max}-I_{min})}$, and $I_{max,(min)}$ are the maximal (minimal) pixel values of the image. The specific choice of $x(I_i, I_j)$ and of $F(x)$ is arbitrary [Wang and Terman, 1997] as long as F is kept negative for large values of $|I_i - I_j|$ and positive for similar values of I_i and I_j. Our choice was inspired by the BCM model [Bienenstock, Cooper and Munro, 1982]. We find that using such a form of interactions contributes to the binding of neurons that belong to the same object, thus improving segmentation of different objects. An example is shown in Fig. 11.7, where segmentation of 4 objects is obtained.

This form of interaction is quite similar to the one used by Wang and Terman [Wang and Terman, 1997], who work with phase-coupled nonlinear oscillators. They name their model LEGION, implying local excitation and global inhibition. Since a previous version of their model [Terman and Wang, 1995] leads to limited temporal segmentation, they have devised an algorithm that allows them to do much better. In their model they have introduced complex lateral interactions that may

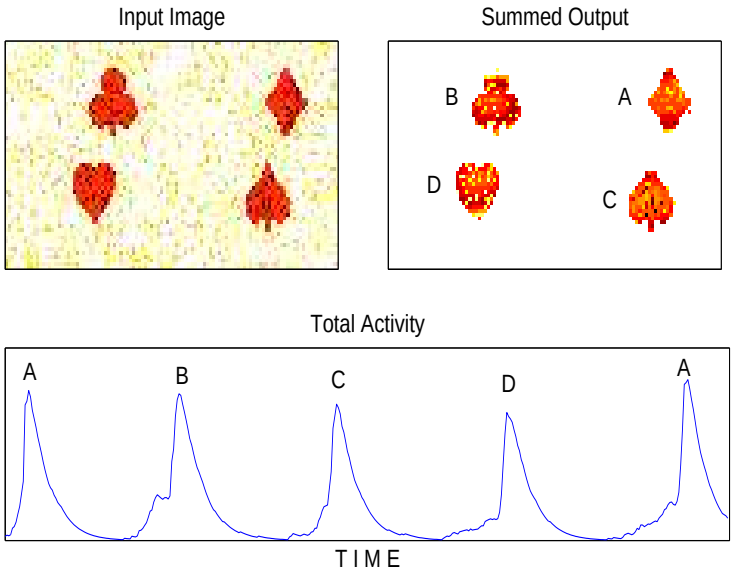

Figure 11.7: Segmentation of 4 non-spherical objects using input dependent connections restricted to a circle of radius 9 around each neuron. The peaks in total activity, shown in the bottom frame, correspond to separate activation of each one of the four objects that are displayed together in the upper right frame. Temporal segmentation is achieved through global inhibition.

shunt the input to an oscillator. These interactions allow for the definition of leading oscillators, that are the elements prone to lateral excitation, which play key roles in forming clusters or segments. The algorithm builds on the general characteristics of nonlinear oscillatory dynamics, but does not follow the same temporal development. In particular, once a segment is activated it may be prevented from firing again until all other segments are activated. As a result, they are able to achieve high degrees of segmentation in images of natural scenes and of medical interest.

Johnson [Johnson, 1994] studied the use of pulse-coupled neural networks for image analysis. His model is inspired by the linking field neural network of [Eckhorn *et al.* , 1990]. It is much more complex than the networks that we use in this chapter. He shows that the frequency histogram of the total activity of his system is stimulus specific. With a certain parameter choice, this histogram can be insensitive to translation and scaling of an object. Implementation of the network as a hybrid optical system yields temporal image segmentation as a result of weak linking between neurons whose thresholds depend dynamically on their own outputs. A similar network is used by [Lindblad *et al.* , 1997] to perform image analysis, where the interaction

between two neurons is inversely proportional to their distance. Noise reduction is done by changing the input to a neuron that is not synchronized with its neighbors. The amount of change depends on the time lag between the firings of the neuron and those of its neighbors. This method produces segmentation whose character changes during the temporal development of the system. Moreover, it also leads to edge detection. The edges of a segment are activated in the iteration that follows the activation of the segment, due to the linking between the perimeter neurons and their neighbors that did not fire. Note that pulse-coupled networks are able to perform both segmentation and edge detection, whereas, so far, only segmentation was implemented by phase-coupled oscillators.

11.5.2 Edge detection

The problem of edge detection is complementary to that of segmentation. Whereas segmentation implies finding areas that belong together, edge detection finds the borderlines between such areas. Edge detection is an important task of image analysis. In various applications, such as in medicine, defining the boundaries of elements in a picture is crucial.

To confront this problem we find it useful to start with synaptic couplings that are not structured by the data. A good candidate is the difference-of-gaussians (DOG) interaction

$$w_{ij} = C_E e^{-d_{ij}^2/d_E} - C_I e^{-d_{ij}^2/d_I}. \tag{11.12}$$

Here d_{ij} is the distance between two points and we have four constants denoting the strength and radii of excitation and inhibition. Since the interactions are symmetric, it is only reasonable that the temporal evolvement of the spiking activity will reflect asymmetries that exist in the input. We find, indeed, that when an image is used as an input then, after the firing pattern settles into a periodic structure, edges can be read off at minima of the total activity.

An example of such behavior can be seen in Fig. 11.8, where the edges of most shaded areas in a SPECT (single photon emission computed tomography) brain image[2] are detected, at time steps that correspond to minima of the total activity of the system. In this analysis we have not employed global inhibition and, therefore, we do not obtain temporal segmentation. At peaks of the total activity, many areas of the image will be active. Nonetheless, using the delineation of boundaries that is observed at minima, we obtain a highly segmented picture.

[2] Image provided by I. Prohovnik, private communication

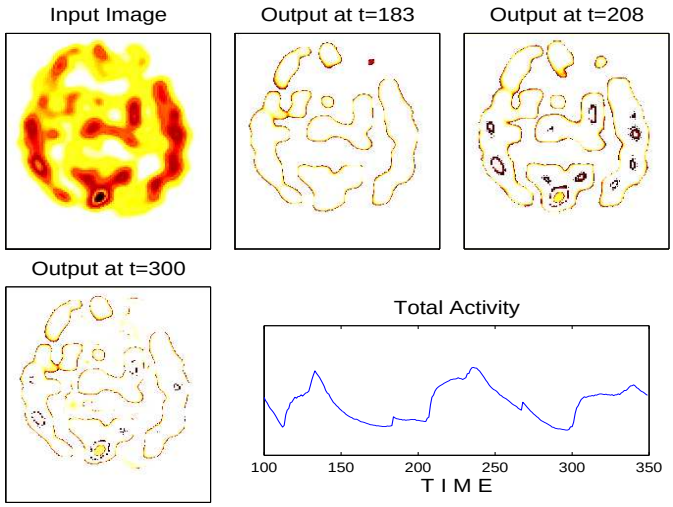

Figure 11.8: Edge detection in a SPECT brain image. The edges of most shaded areas appear at different local minima of the total activity. The behavior of the activity in time is rather complicated, due to the complexity of the input image. Therefore, different combinations of edges appear at time steps that correspond to different minima of the total activity of the system.

11.6 Solitary Waves

Wilson and Cowan [Wilson and Cowan, 1973] have realized that if one builds aggregates of neurons one may naturally obtain the formation of unattenuated traveling waves as a result of a localized input. Studying two dimensional layers of interacting neurons, [Ermentrout and Cowan, 1979] have observed formations of moving stripes. They have pointed out that if their model is applied to V1, it can provide an explanation of drug-induced visual hallucinations, relying on the retinocortical map interpretation of V1. In a more recent work using spiking neurons, [Föhlmeister *et al.* , 1995] have obtained, in addition to stripe formations, rotating spirals, expanding concentric rings and collective bursts. Most of these coherent excitations, whose structure is continuous in space and time, can be characterized as solitary waves [Meron, 1992]. They move in space with some well defined speed, or expand from, or rotate around, some focus. This holds until they meet some other wave-front of similar character, in which case they annihilate one another.

In the present section we provide some examples of this behavior and explain the topologic character of the resulting solitary waves. In our analysis we employ a constant input for the whole surface of neurons. In the absence of any interactions

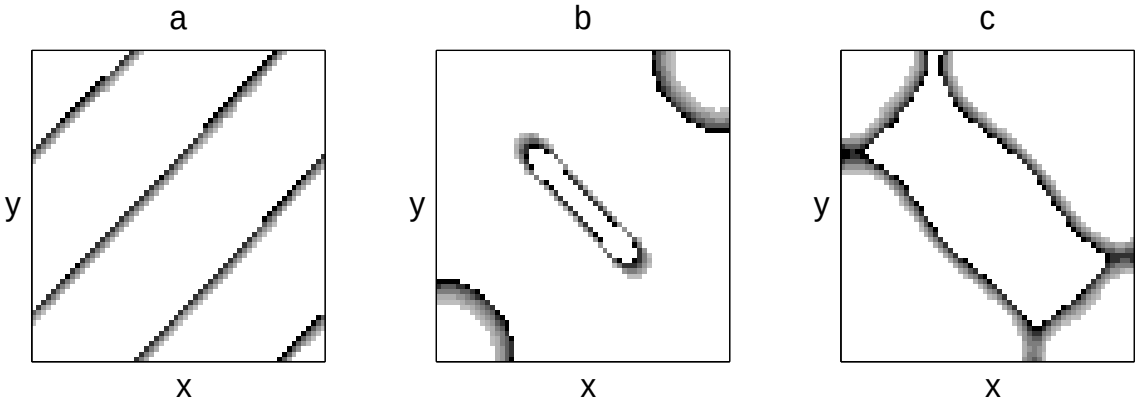

Figure 11.9: Two solutions with propagating spiking fronts (the grey scale is proportional to the strength of f_i) on a 60×60 grid using the same interaction parameters. (a) Periodic boundary conditions lead to parallel stripes. Frames (b) and (c) display two snapshots of a solution corresponding to open boundary conditions. In (b) we see two arcs propagating from opposite corners, merging in (c) with fronts that started in the other corners, to form a rectangle that eventually shrinks to the structure seen in the center of (b). Interaction parameters are $C_E = 0.2$, $C_I = 0.02$, $d_E = 15$, $d_I = 100$, restricted to an area of radius 20 around each neuron. Other parameters are the same as in Fig. 11.1.

among the neurons, and starting from random initial conditions, this would lead to random periodic behavior of the type of Fig. 11.2b. This changes once we introduce an interaction such as in Eq. 11.12. For strong enough simultaneous excitations the system develops a coherent character, i.e. neighboring neurons become synchronized, thus leading to spatial order. The system turns then into a structured cyclic attractor. The details of the structure depend in a critical manner on the interaction parameters.

In Fig. 11.9 we display results of propagating stripes, as well as formations of merging lines. When viewed at different time frames one observes a homogeneous motion of these structures. The two formations represent the same type of solution, namely propagating fronts. They were obtained with the same set of interaction parameters, but with different boundary and initial conditions. The parallel stripes of Fig. 11.9a are the result of periodic boundaries and the merging lines of Fig. 11.9b and c are the result of open boundaries. The latter cause the activity to start at boundary neurons, that receive less inhibition than others. The convergence onto a specific solution depends on initial conditions of the complex nonlinear system. The distinction between solutions belonging to periodic or open boundary conditions is always quite evident.

Rotating spirals and expanding rings are other types of solutions, that are well known examples of solitary wave formations [Meron, 1992]. Both formations are often encountered in 2-d arrays of IAF neurons [Jung and Mayer-Kress, 1995, Milton, Chu and Cowan, 1993]. An example of colliding rings is displayed in Fig. 11.10. This example is obtained by keeping only few nearby neighbors in the interaction. The number of expanding rings is inversely related to the span of the interactions. We note the spontaneous creation of two foci from which the expanding rings emerge. Spikes exists only at the boundary between $m = 0$ and $m = 1$ areas. This property reflects the fact that for each neuron a spike is followed by a refractory period. It is responsible for the vanishing of two firing fronts that collide, because, after collision, there remains only a single $m = 0$ area, formed by the merger of the two former $m = 0$ areas.

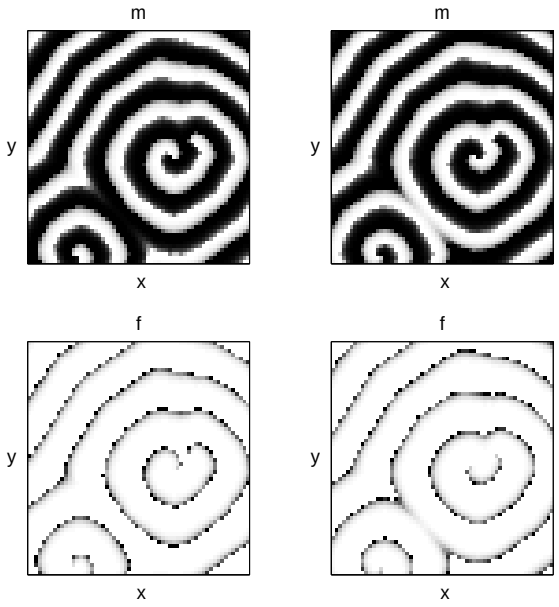

Figure 11.10: Collision of two expanding rings formed on a 60×60 grid. The top frames display m fields at two time steps, with $m = 0$ in white and $m = 1$ in black. The bottom frames exhibit the corresponding coherent firing patterns, that appear at boundaries between areas of $m = 0$ and $m = 1$. In this simulation we use excitatory interactions only, coupling each neuron to its 8 neighbors with an amplitude of 0.3.

All these simulations are carried out on some finite lattice, containing typically 60×60 IAF neurons. Once the system adapts to its coherent behavior, the structure of its underlying lattice becomes unimportant. In fact, it turns into a continuous problem of interacting neural fields. There is a topologic rule that we can deduce

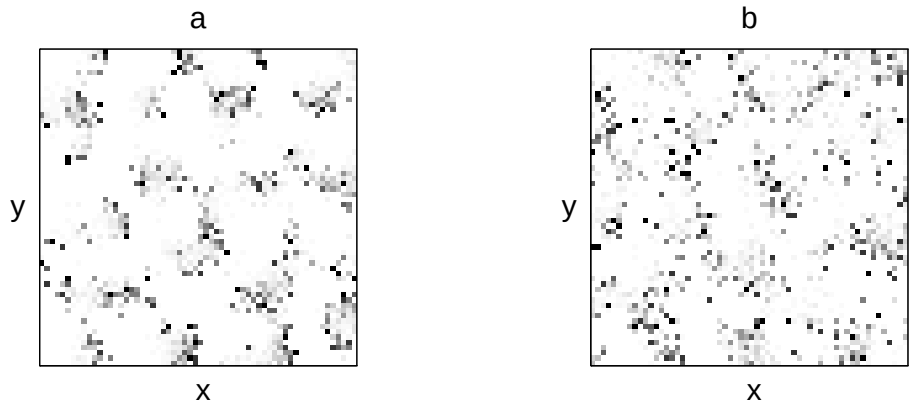

Figure 11.11: Incoherent firing patterns for (a) high variability of synaptic connections, or (b) noisy input. In (a) we have multiplied 75% of all synapses by a random gaussian component (mean=1., s.d=3.) that stays constant in time. In (b) we have employed a noisy input that varies in space and time (mean=0.29, s.d.=0.25). In both frames the firing patterns are no longer coherent. We can see the formation of small clusters of spiking neurons. The typical length scale of these patches is of the order of the span of excitatory interactions. This is a manifestation of the dominance of interactions in determining the spatial behavior in the absence of continuity that imposes the topologic constraint.

from this continuity. Once $m(\vec{x},t)$ is continuous, it has the same dimensionality D (2 in the cases discussed here) as the manifold to which the neurons are attached. Since all firing formations occur at moving fronts of $m(\vec{x},t) = 1$ patches, these solitary waves have to be of dimensionality $D-1$. This is well exemplified in Fig. 11.10. It holds for all the coherent solutions that we obtain, arcs, spirals, stripes and expanding rings.

We have obtained coherent solutions also when some forms of synaptic delays were introduced. Coherence can be broken by strong noise in the input or by randomness in the synaptic connections. What we would expect in this case is that the DOG interactions specify the resulting behavior of the system. This is, indeed, the case, as demonstrated in Fig. 11.11 which shows an irregular, but patchy, behavior. These patches have a typical length scale that is of the order of the range of excitatory interactions. We believe that this is the explanation for the moving patches of activity reported by other authors [Hill and Villa, 1994, Usher *et al.* , 1994]. These are incoherent phenomena, emerging in models with randomly distributed radial connections.

We learn therefore that our model embodies two competing factors. The DOG interactions tend to produce patchy firing patterns, but the coherence, that is brought about by the excitatory connections, leads to the formation of one dimensional solitary waves on a two dimensional manifold. If, however, strong fluctuations exist, i.e. the neurons can no longer be described by homogeneous physiological and geometrical properties, the resulting patterns of firing activity are incoherent, and their spatial extension reflects the range of the underlying interactions.

Are there situations where coherent firing activity exists in neuronal tissue? If the explanation of hallucinatory phenomena [Ermentrout and Cowan, 1979] is correct, then this is expected to be the case. It could be proved experimentally through optical imaging of V1 under appropriate pharmacological conditions. Other abnormal brain activities, such as epileptic seizures, could also fall into the category of coherent firing patterns. Does coherence occur also under normal functioning conditions? The interesting spatiotemporal evoked activity, reported by [Arieli *et al.* , 1996] in areas 17 and 18 in cat, may be due to underlying neurons that fire incoherently. But the thalamo-cortical spindle waves generated by the reticular thalamic nucleus [Golomb, Wang and Rinzel, 1994, Contreras and Steriade, 1996] may well be an example of coherent activity. Another example could be the synchronous bursts of activity that propagate as wave fronts in retinal ganglion cells of neonatal mammals [Meister *et al.* , 1991, Wong, 1993]. It has been suggested that these waves play an important role in the formation of ocular dominance layers in the LGN [Meister *et al.* , 1991].

11.7 The Importance of Noise

The effects of noise, displayed in Fig. 11.11, are deconstructive, in the sense that noise causes desynchronization and, therefore, eliminates the coherent behavior. However, desynchronization may also have useful aspects, as seen in section 11.4 and displayed in Fig. 11.6, where noise helped us to overcome temporal segmentation constraints. This observation goes back to [Horn, Sagi and Usher, 1991], where it was shown that noise can serve the binding process by forming a nucleation source for synchronization of one segment. As such it can serve also in image segmentation analysis [Wang and Terman, 1997].

It is interesting that, under certain conditions, noise can also be employed to allow for solitary wave formation, rather than destroy it. This is the case in a dissipative regime in which the IAF neurons do not have a constant input that keeps them oscillating, as already noted by [Jung and Mayer-Kress, 1995]. A one dimensional

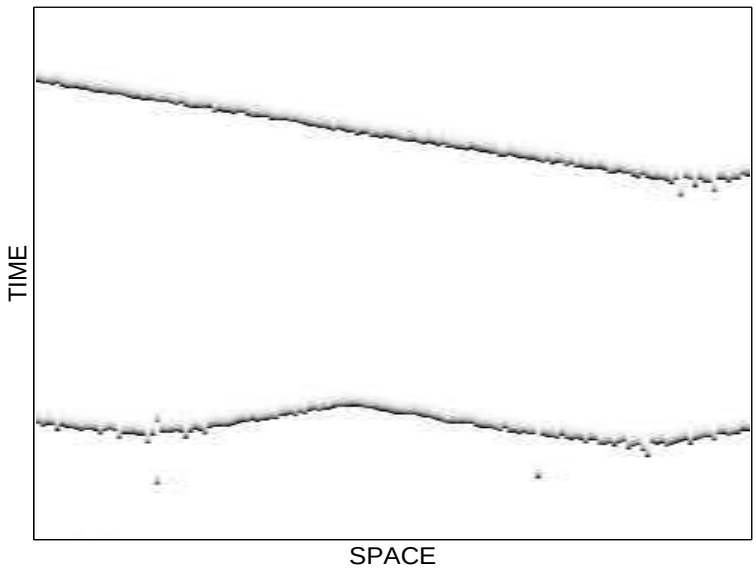

Figure 11.12: Space time description of coherent spiking activity on a one dimensional neural manifold in a dissipative regime. The coherent propagation of excitation, induced by random inputs, is similar to what is observed in the oscillatory regime, except that it is not periodic and less frequent. Parameters are: $w = 1.2$ for 10 neighbors on each side. I is normally distributed with mean and standard deviation of 0.02. Its values change at random time steps.

example [Horn and Opher, 1997b] of such a system is shown in Fig. 11.12. Once a neuron fires, the spreading of activity depends on the situation of near-by neurons. If they happen to be in a refractory period, or under the influence of small, or even negative input, activation will not spread. However, once activation does spread, it behaves in the same way as in the oscillatory regime. In this one dimensional example we observe creation and annihilation of solitary waves. Note that this system can no longer have the global periodic structure that is characteristic of the oscillatory regime.

Note that in this example noise serves only as the source of energy for the system to excite itself, and it is not strong enough to break the underlying homogeneous structure. If we strengthen it considerably we will end up again with the type of behavior displayed in Fig. 11.11.

11.8 Conclusions

Using synchrony of spiking neurons, we have analyzed different cases of coherent firing activity that lead to interesting spatiotemporal formations. These phenomena can be employed for clustering of data consisting of a few tens of elements and ranging up to ten thousand elements, as is the case for image segmentation.

Our analysis was carried out on a fairly simple system. It could, therefore, serve as a general framework within which we attack a wide scope of problems, covering clustering (section 11.3), image segmentation (section 11.5.1), edge detection (section 11.5.2) and formation of solitary waves (section 11.6). Emphasizing the generality of the method, we inevitably lose on its ability to lead in the technical application frontier over other specialized techniques.

One of the main features of temporal segmentation with non-linear oscillators is the inherent limit that we discussed in section 11.4. This limit constrains our general analysis of clustering, and limits our ability to perform image segmentation. In order to have better designs for application purposes one has to find tricks to overcome this limit, using methods that are no longer motivated by biological intuition. It is satisfying to note that limited segmentation is characteristic of human ability to process simultaneously different streams of data.

If we try to define the type of computational tasks that our system performs, the appropriate classification would be feature extraction. Conventional neural computation techniques that are being used for such purposes are based on unsupervised competitive learning. Such learning was not performed in our model, although in principle it could be added to it. We have used throughout this chapter fixed synaptic weights. However competition was built into our system, often through explicit inhibitory actions. The winner-take-all feature of the conventional techniques of unsupervised learning, is replaced in our models by the dominance of a particular cluster during a specific time frame. In other words, temporal segmentation is a way of breaking a given problem (or data set) into several clusters such that each one becomes a winner sometimes. By performing computation along the time axis, we are able to carry out feature extraction without a training algorithm.

Finally let us emphasize that the coherent behavior described in this chapter is quite robust, as long as the underlying system of spiking neurons is homogeneous and its interactions are suitable for mutual synchronization. The interesting spatiotemporal properties of such systems may play an important role in pattern analysis and pattern formation in both biological and artificial neural systems.

Acknowledgment

This work was partly supported by the Israel Science Foundation.

Bibliography

[Abbott and van Vreeswijk, 1993] Abbott, L.F. and van Vreeswijk, C. (1993). Asynchronous states in networks of pulse-coupled oscillators. *Physical Rev. E* 48, 1483–1490.

[Arieli *et al.* , 1996] Arieli, A., Sterkin A., Grinvlad A. and Aertsen A (1996). Dynamics of ongoing activity: explanation of the large variability in evoked responses. *Science* 273, 1868–1871.

[Bienenstock, Cooper and Munro, 1982] Bienenstock, E.L., Cooper, L.N. and Munro, P.W. (1982). Theory for the development of neuron selectivity: orientation specificity and binocular interaction in visual cortex. *The J. of Neurosci.* 2, 32–48.

[Blatt, Wiseman and Domany, 1997] Blatt, M., Wiseman, S. and Domany, E. (1997). Data clustering using a model granular magnet. *Neural Computation* 9, 1805–1842.

[Contreras and Steriade, 1996] Contreras, D. and Steriade, M. (1996). Spindle oscillation in cats: the role of corticothalamic feedback in a thalamically generated rhythm. *J. of Physiology* 490, 159–179.

[Crook, Ermentrout and Bower, 1997] Crook, S. M., Ermentrout, G. B. and Bower, J. M. (1997). Spike frequency adaptation affects the synchronization properties of networks of cortical oscillators. *Comp. Neurosc. Meeting, CNS*97,* Big-Sky MO.

[Eckhorn *et al.* , 1988] Eckhorn, R., Bauer, R., Jordan, W., Brosch, M., Kruse, W., Munk, M., and Reitboeck, H. J. (1988). Coherent oscillations: a mechanism of feature linking in the visual cortex? In:*Biol. Cybern.* 60, 121–130.

[Eckhorn *et al.* , 1990] Eckhorn, R., Reitboeck, H.J., Arndt, M. and Dicke, P. (1990). Feature linking via synchronization among distributed assemblies: simulations of results from cat visual cortex. *Neural Comp.* 2, 293–307.

[Ermentrout and Cowan, 1979] Ermentrout, G.B. and Cowan J.D. (1979). A mathematical theory of visual hallucination patterns.*Biol. Cyb.* 34, 136–150.

[Duda and Hart, 1973] Duda, R. O. and Hart, P. E. (1973). *Pattern classification and scene analysis*. New York, Wiley-Interscience.

[Föhlmeister *et al.* , 1995] Föhlmeister, C., Gerstner, W., Ritz, R. and van Hemmen, J. L. (1995). Spontaneous excitation in the visual cortex: stripes, spirals, rings and collective bursts. *Neural Comp.* 7, 905–914.

[Gerstner, Ritz and van Hemmen, 1993] Gerstner, W. Ritz, R. and van Hemmen, J.L. (1993). A biologically motivated and analytically soluble model of collective oscillations in the cortex I. Theory of weak locking. *Biol. Cybern.* 68 363–374.

[Gerstner, van Hemmen and Cowan, 1996] Gerstner, W., van Hemmen, J.L. and Cowan, J.D. (1996). What matters in neuronal locking. *Neural Comp.* 8, 1653–1676.

[Golomb *et al.* , 1992] Golomb, D. Hansel, D. Shraiman, S. and Sompolinsky, H. (1992). Clustering in globally coupled phase oscillators. *Physical Rev. A.* 45, 3516–3530.

[Golomb, Wang and Rinzel, 1994] Golomb, D., Wang, X.J. and Rinzel, J. (1994). Synchronization properties of Spindle oscillations in a thalamic reticular nucleus model. *J. of Neurophys.* 72, 1109–1126.

[Grannan, Kleinfeld and Sompolinsky, 1993] Grannan, E.R., Kleinfeld, D. and Sompolinsky, H. (1993). Stimulus-dependent synchronization of neuronal assemblies. *Neural Comp.* 5, 550–569.

[Gray *et al.* , 1989] Gray, C.M., König, P., Engel, A.K. and Singer, W. (1989). Oscillatory responses in cat visual cortex exhibit inter-columnar synchronization which reflects global stimulus properties. *Nature* 338, 334–337.

[Hansel, Mato and Meunier, 1995] Hansel, D. Mato, M. and Meunier, C. (1995). Synchrony in excitatory neural network. *Neural Comp.* 7, 307–337.

[Hill and Villa, 1994] Hill, S.L. and Villa, A.E.P. (1994). Global spatio-temporal activity influenced by local kinetics in a simulated "cortical" neural network. In:*Supercomputing in brain research: From tomography to neural networks / workshop on supercomputing in brain research.* Eds: H.J. Herrmann, D.E. Wolf and E. Poppel. World Scientific.

[Horn and Usher, 1991] Horn,D. and Usher,M. (1991). Parallel activation of memories in an oscillatory neural network. *Neural Computation* 3, 31–43.

[Horn, Sagi and Usher, 1991] Horn,D., Sagi,D. and Usher,M. (1991). Segmentation, Binding and Illusory Conjunctions. *Neural Computation* 3, 510–525.

[Horn and Usher, 1992] Horn,D., and Usher, M. (1992). Oscillatory model of short term memory, in *Advances in Neural Information and Processing Systems 4*, J.E.Moody S.J.Hanson R.P.Lippmann eds,(Morgan Kaufmann Pub.) p. 125-132.

[Horn and Opher, 1996a] Horn, D. and Opher, I. (1996). Temporal Segmentation in a Neural Dynamical System. *Neural Comp.* 8, 375–391.

[Horn and Opher, 1996b] Horn, D. and Opher, I. (1996). The Importance of Noise for Segmentation and Binding in Dynamical Neural Systems. *Int. Journal of Neural Systems,* 7, 529–535.

[Horn and Opher, 1997a] Horn, D. and Opher, I. (1997). Solitary waves of integrate and fire neural fields *Neural Comp.* 9, 1677–1690.

[Horn and Opher, 1997b] Horn, D. and Opher, I. (1997). Solitary Waves on Manifolds of Integrate-and-Fire Neurons. To be published in *Phyl. Mag. B, Proceedings of the Minerva workshop on Mesoscopics, Fractals and Neural Networks,*.

[Hopfield and Herz, 1995] Hopfield, J.J. and Herz, A.V.M. (1995). Rapid local synchronization of action potentials: toward computation with coupled integrate-and-fire neurons *PNAS* 92, 6655–6662.

[Johnson, 1994] Johnson, L.J. (1994). Pulse-coupled neural nets: translation, rotation, scale, distortion and intensity invariance for images. *App. Optics* 33, 6239–6253.

[Jung and Mayer-Kress, 1995] Jung, P. and Mayer-Kress, G. (1995). Noise controlled spiral growth in excitable media. *Chaos*, 5, 458–462.

[Kuramoto, 1990] Kuramoto, Y. (1990). Collective synchronization of Pulse-coupled oscillators and excitable units. *Physica D* 50, 15–30.

[Lindblad *et al.* , 1997] Lindblad, Th., Becanovic V., Lindsey C.S. and Szekely, G. (1997). Intelligent detectors modelled from the cat's eye. *Nuclear Instruments and Methods in Physics Research* A, 389, 245–250.

[von der Malsburg, 1981] von der Malsburg, C. (1981). The correlation theory of brain function. Internal Report 81-2, Max-Planck-Institute for Biophysical Chemistry. Reprinted in *Models of Neural Networks II,* Domany *et al.* (Eds.), Springer, 1994, 95–119.

[von der Malsburg and Schneider, 1986] von der Malsburg, C. and Schneider, W. (1986). A neural cocktail party processor. *Biol. Cybern.* 54, 29–40.

[von der Malsburg and Buhman, 1992] von der Malsburg, C. and Buhman, J. (1992). Sensory segmentation with coupled neural oscillators. *Biol. Cybern.* 67, 233–242.

[Meister *et al.* , 1991] Meister M., Wong R.O.L., Denis A.B. and Shatz C.J. (1991). Synchronous bursts of action potentials in ganglion cells of the developing mammalian retina. *Science* 252, 939–943.

[Meron, 1992] Meron, E. (1992). Pattern formation in excitable media. *Physics Reports* 218, 1–66.

[Miller, 1956] Miller,G.A. (1956). The magical number seven, plus or minus two: Some limits on our capacity of processing information. *Psychological Rev.* 63, 81–97.

[Milton, Chu and Cowan, 1993] Milton, J.G., Chu, P.H. and Cowan, J.D. (1993). Spiral waves in integrate-and-fire neural networks. in Advances in *Neural Information Processing Systems* (eds. Hanson, S.J., Cowan, J.P. and Giles, C.L.) 5, 1001–1007.

[Mirollo and Strogatz, 1990] Mirollo, R.E. and Strogatz, S.H. (1990). Synchronization of pulse-coupled biological oscillators *SIAM J. Appl. Math.* 50, 1645–1662.

[Nischwitz and Glünder, 1995] Nischwitz, A. and Glünder, H. (1995). Local lateral inhibition: a key to spike synchronization? *Biol. Cybern.* 73, 389–400.

[Ritz *et al.* , 1994] Ritz, R., Gerstner, W. Feuntes, U. and van Hemmen, J.L. (1994). A biologically motivated and analytically soluble model of collective oscillations in the cortex II. Application to binding and pattern segmentation. *Biol. Cybern.* 71, 349–358.

[Strogatz and Stewart, 1993] Strogatz, S.H. and Stewart, I (1993). Coupled oscillators and biological synchronization *Scientific American* Dec. 93, 68–75.

[Strogatz and Mirollo, 1988] Strogatz, S.H. and Mirollo R.E. (1988). Phase locking and critical phenomena in lattices of coupled nonlinear oscillators with random intrinsic frequencies. *Physica D.* 31 143–168.

[Terman and Wang, 1995] Terman, D. and Wang, D.L. (1995). Global competition and local cooperation in a network of neural oscillators. *Physica D* 81, 148–176.

[Usher, Schuster and Niebur, 1993] Usher, M., Schuster, H.S., and Niebur, E. (1993). Dynamics of populations of integrate-and-fire neurons, partial synchronization and Memory. *Neural Comp.* 5, 570–586.

[Usher *et al.* , 1994] Usher, M., Stemmler, M., Koch, C. and Olami., Z. (1994). Network Amplification of local fluctuations causes high spike rate variability, fractal firing patterns and oscillatory local field potentials. *Neural Comp.* 6, 795–836.

[van Vreeswijk and Abbott, 1994] van Vreeswijk, C. and Abbott, L.F. (1994). When inhibition not excitation synchronizes neural firing *J. of Comp. Neurosci.* 1, 313–321.

[van Vreeswijk and Hansel, 1997] van Vreeswijk, C. and Hansel, D. (1997). Rhythmic bursting in networks of adaptive spiking neurons. *Comp. Neurosc. Meeting, CNS*97*, Big-Sky MO.

[Wang, Buhman and von der Malsburg, 1990] Wang, D., Buhman, J. and von der Malsburg, C. (1990). Pattern segmentation in associative memory. *Neural Comp.* 2, 94–106.

[Wang and Terman, 1997] Wang, D. and Terman, D. (1997). Image Segmentation Based on Oscillatory Correlation. *Neural Comp.* 9. 805–836; Err: 9, 1623–1626.

[Wilson and Cowan, 1973] Wilson, H.R. and Cowan, J.D. (1973). A mathematical theory of the functional dynamics of cortical and thalamic nervous tissue. *Kybernetik* 13, 55–80.

[Wong, 1993] Wong R.O.L. (1993). The role of spatio-temporal firing patterns in neuronal development of sensory systems. *Curr. Op. Neurobio* 3, 595–601.